Wave-particle dualism and complementarity unraveled by a different mode

Ralf Menzel[a,1], Dirk Puhlmann[a], Axel Heuer[a], and Wolfgang P. Schleich[b]

[a]Photonik, Institut für Physik und Astronomie, Universität Potsdam, D14476 Potsdam, Germany; and [b]Institut für Quantenphysik and Center for Integrated Quantum Science and Technology, Universität Ulm, D89069 Ulm, Germany

Edited by* Marlan O. Scully, Texas A&M and Princeton Universities, College Station, TX, and Princeton, NJ, and approved April 16, 2012 (received for review January 23, 2012)

The precise knowledge of one of two complementary experimental outcomes prevents us from obtaining complete information about the other one. This formulation of Niels Bohr's principle of complementarity when applied to the paradigm of wave-particle dualism—that is, to Young's double-slit experiment—implies that the information about the slit through which a quantum particle has passed erases interference. In the present paper we report a double-slit experiment using two photons created by spontaneous parametric down-conversion where we observe interference in the signal photon despite the fact that we have located it in one of the slits due to its entanglement with the idler photon. This surprising aspect of complementarity comes to light by our special choice of the TEM_{01} pump mode. According to quantum field theory the signal photon is then in a coherent superposition of two distinct wave vectors giving rise to interference fringes analogous to two mechanical slits.

The double-slit experiment has served as a source of inspiration for more than two centuries. Indeed, Thomas Young (1) has used it to argue in favor of the wave theory of light rather than the corpuscular one of Isaac Newton (2). In the early days of quantum mechanics it was central to the dialogue (3) between Albert Einstein and Bohr on epistemological problems in atomic physics. Moreover, it was the starting point of the path integral formulation (4) of quantum mechanics by Richard Feynman.

Today the question of "which-slit" versus "interference" in the double-slit configuration (5) is as fascinating and relevant (6) as it was in the early days of quantum mechanics. In particular, the understanding of the physical origin (7) of the disappearance of the fringes in the presence of which-slit information has come a long way. Werner Heisenberg in the context of the uncertainty relation (8), Bohr in his discussion with Einstein (3) on the recoiling slit, and others (9) have argued in favor of an uncontrollable momentum transfer (7). However, the Gedanken experiments of the quantum eraser (10) and the micromaser "welcher Weg" detector (11) have identified entanglement and the availability of information as the main culprit. Indeed, the seminal atom interferometer experiment (12) as well as the realization (13) of the quantum eraser have made a clear decision against momentum transfer in favor of entanglement. As a result, today the principle of complementarity (14) is widely accepted (15) in the form (16):

> "If information on one complementary variable is in principle available even if we choose not to 'know' it… we will lose the possibility of knowing the precise value of the other complementary variable."

In the present paper we report the results of a double-slit experiment that brings out an additional layer of this principle. We employ the entanglement between the signal and the idler photon created in spontaneous parametric down-conversion (SPDC) (17) to obtain by a coincidence measurement of the two photons which-slit information about the signal photon without ever touching it. Moreover, we observe in a separate coincidence experiment interference fringes in the signal photon. This result is surprising because which-slit information about the signal photon is "available" and therefore the principle of complementarity suggests no interference. The explanation of this puzzling experimental observation springs from the transverse mode structure of the pump with two intensity maxima that creates a superposition of two macroscopically distinguishable wave vectors of the signal photon. In the case of a Gaussian pump with a single maximum no such superposition arises (18).

Our Experiment

We now briefly describe our experimental setup and then discuss our results. For a more detailed description of this experiment we refer to *Materials and Methods*.

Experimental Setup. In contrast to the standard arrangement of SPDC in our experiment summarized in Fig. 1 the pump laser was in the TEM_{01} mode, which displays two distinct maxima. The resulting two intensity maxima of signal and idler photon at the exit of the beta barium borate (BBO) crystal are imaged with the help of a lens and a polarizing beam splitter (PBS) onto the two slits of a double-slit and onto a single-photon counting detector* D1. Because the distances from the fiber of D1 to PBS and from the double-slit to PBS are identical the two light spots of the signal photons in the two slits are identical to the two spots of the idler photon on D1. Moreover, the intensity of the pump beam is low enough to ensure that only one photon pair was created at a measuring time interval.

We have first recorded the intensity distribution shown in Fig. 2 using an electron multiplying charge coupled device (EMCCD) camera (Ixon 897, Andor) placed at the position of the double-slit. The individual pixels of size 16 μm × 16 μm are clearly visible in the picture. Moreover, the intensity in the centerline is not exactly zero, which most likely is due to imperfections of the imaging.

Which-Slit Information. Next we demonstrate that the entanglement between signal and idler photon provides us with which-slit information. For this purpose we replace the EMCCD camera by the double-slit and put another detector D2 on a motorized translation stage behind the double-slit. With this arrangement the near-field correlations between the signal and the idler photons depicted on the lower right of Fig. 3 were obtained as a function of the vertical and horizontal position of D2. Throughout these measurements the location of D1 was fixed either inside the upper or lower spot of the TEM_{01} mode structure as indicated by the two magnifying glasses on the left side of the figure. The

Author contributions: R.M. designed research; R.M., D.P., A.H., and W.P.S. performed research; and R.M. and W.P.S. wrote the paper.

The authors declare no conflict of interest.

*This Direct Submission article had a prearranged editor.

Freely available online through the PNAS open access option.

*As single-photon counting modules we employ PerkinElmer SPCM-AQR-15 avalanche photo diodes coupled by a multimode graded index fiber of a core diameter 62.5 μm

[1]To whom correspondence should be addressed. E-mail: photonics@uni-potsdam.de.

Downloaded from https://www.pnas.org by 3.238.227.73 on September 20, 2024 from IP address 3.238.227.73.

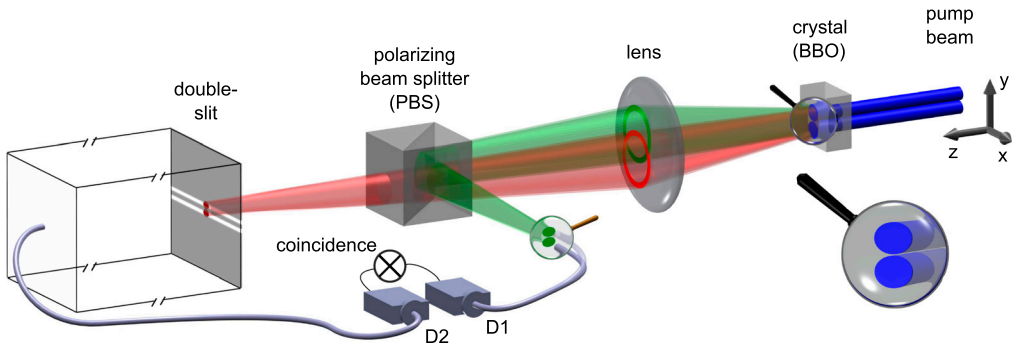

Fig. 1. Artist's view of our experimental setup for the simultaneous observation of which-slit information and interference in Young's double-slit experiment. We pump a nonlinear crystal (BBO) with a laser (blue) in a mode (TEM_{01}) with two distinct maxima and separate the emerging signal (red) and idler (green) photons by a polarizing beam splitter (PBS). A lens images the two intensity maxima at the exit of the crystal shown by the magnifying glass on the right onto the two openings of the double-slit (signal photon) or onto the plane of the detector D1 (idler photon). We observe in coincidence the signal and the idler photon. The detector D2 is located either just behind, or far away from, the two slits.

origin of the *y* axis is not halfway between the two slits but is determined by the scale of the translation stage.

The evaluation of the experimental data yields a contrast ratio of about 1% cross correlation photons. Thus, from all the photons measured behind the slit in coincidence with the reference detector, at least 99% were passing through the related slit (upper-upper or lower-lower), and only 1% in maximum passed through the other slit (upper-lower or lower-upper) as a result of measurement errors. This experimental result confirms that photons measured in coincidence with the two selected positions of a reference detector are passing with at least 99% probability just through the one selected slit.

Interference and Which-Slit Information. Next we have performed the which-slit and interference correlation experiment outlined in Fig. 4. We have moved the detector D2 into the far field of the double-slit and have measured as a function of its vertical position the signal photons in coincidence with the idler photons recorded on D1 positioned in this experiment at the lower spot corresponding to the bottom part of Fig. 3. In the lower part of Fig. 4 we show the results of this coincidence measurement. We emphasize that the interference fringes of the signal photons in the far field of the double-slit are clearly visible while from the measurement of the idler photon probing the near field we also obtain the related which-slit information. Indeed, because in this case D1 was placed onto the lower spot the signal photon must have gone through the lower slit. We note that our results are in good agreement with the prediction (solid line) based on the standard double-slit far-field intensity formula discussed in *Materials and Methods*.

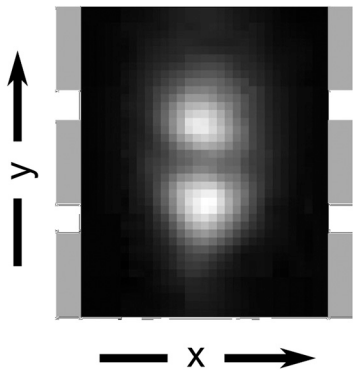

Fig. 2. Intensity of the signal photons on an EMCCD camera at the position of the double-slit. Because measurements with the EMCCD camera and the double-slit at the same position are mutually exclusive we can only infer the approximate location of the slits indicated by the shaded area relative to the TEM_{01} mode. The height and width of this figure correspond to 624 μm and 496 μm, respectively (39 × 31 pixel).

First-Order Single-Photon Interference. Finally, we have taken pictures of the interference pattern formed by the signal photons in the far field of the double-slit with the EMCCD camera. We emphasize that in this case we do not measure in coincidence with the idler photons; that is, we collect all signal photons with-

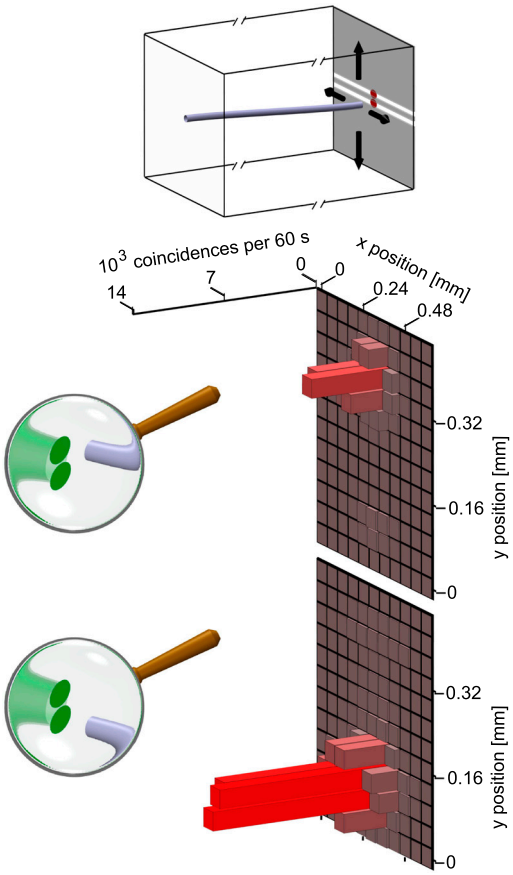

Fig. 3. Which-slit information in Young's double-slit experiment obtained via the entanglement between the signal and idler photon. The detector D2 is scanned in the *x*-*y* plane of the near field behind the two slits as indicated by the box on the top. Due to the entanglement of the two photons an idler photon measured on the detector D1 that is positioned in the upper or lower intensity maximum as indicated by the two magnifying glasses on the left implies that the signal photon has gone through the upper or lower slit as confirmed by the coincidence measurements on the right.

Downloaded from https://www.pnas.org by 3.238.227.73 on September 20, 2024 from IP address 3.238.227.73.

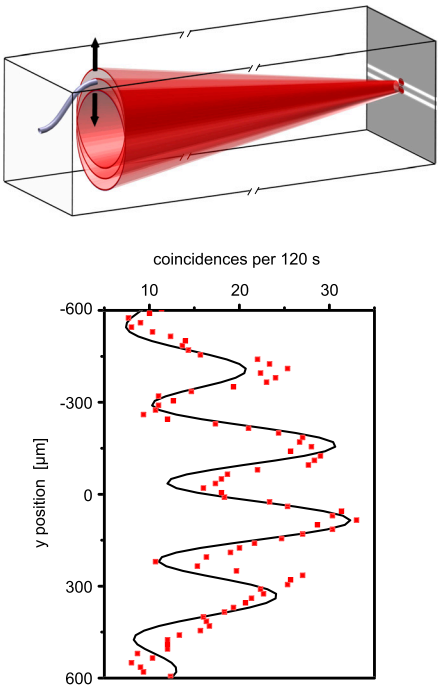

Fig. 4. Coincidence measurements between the signal photon (red) in the far field of the double-slit indicated by the box on the top and the idler photon detected in the lower intensity maximum. Despite this which-slit information (lower slit) the signal photon displays interference fringes shown on the lower part when we scan D2 along the *y* axis in the far field. The solid line is a fit to the data based on the standard double-slit intensity formula discussed in the materials and methods section.

out retaining the which-slit information. Therefore, the principle of complementarity predicts interference of the signal photons, which is confirmed by the right picture of Fig. 5. Here we display the familiar ring structure originating from a vertical cut through the light cone of the signal photons emerging from SPDC. However, we note five interference fringes at the top and the bottom of the ring. On the right and left sides of the ring an averaging of the fringes in the vertical direction takes place. But if one slit is closed the fringes disappear and the diffraction of the signal photon from the single slit gives rise to a broadening of the ring structure on the top and the bottom as shown on the left of Fig. 5.

Theoretical Analysis

In the present section we use the tools of quantum field theory (19) and, in particular, quantum optics (20) to explain the experimental results reported in the preceding section. This discussion brings out most clearly that they are not in contradiction with quantum theory.

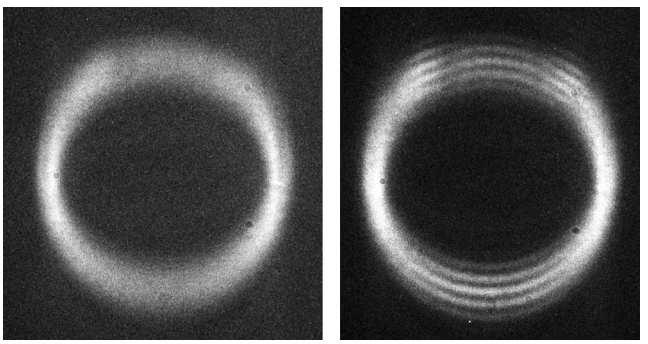

Fig. 5. First-order intensity measurements of the signal photons with an EMCCD camera in the far-field region of the double-slit with both slits open (right) or the upper one closed (left). The signal photon displays interference fringes only when both slits are open, but when one is closed the fringes disappear as suggested by the principle of complementarity.

Superposition of Two Wave Vectors. In *Materials and Methods* we present a model for SPDC motivated by ref. 20 consisting of a gas of stationary three-level atoms of constant density and obtain the quantum state $|\Psi\rangle$ of the two-photon field. The main difference to the expression in ref. 20 is the sum over the positions $\mathbf{R}$ of all atoms weighted by the mode function u and the fact that in our experiment we separate idler and signal photons with the help of their different polarizations. When we take these two differences into account we find the joint probability amplitude

$$w(\mathbf{k}_T^{(s)};\mathbf{k}_T^{(i)}) = \alpha u_0[\delta x(k_x^{(s)} + k_x^{(i)})]u_1[\delta y(k_y^{(s)} + k_y^{(i)})] \qquad [1]$$

to observe the transverse wave vectors $\mathbf{k}_T^{(s)} \equiv (k_x^{(s)}, k_y^{(s)})$ of the signal photon given the transverse wave vector $\mathbf{k}_T^{(i)} \equiv (k_x^{(i)}, k_y^{(i)})$ of the idler photon. Here α is a constant, and u_0 and u_1 denote the two lowest Hermite–Gaussian modes shown in Fig. 6.

Because $u_0 \equiv u_0(\xi)$ has a single maximum at $\xi = 0$ the x components of the wave vectors of the signal and idler photon are preferentially anticorrelated as shown in the left column of Fig. 6—that is, $k_x^{(s)} \cong -k_x^{(i)}$ with a spread $\delta k_x \equiv 1/\delta x$. However, due to the fact that u_1 has maxima at $\xi = \pm 1$ we find from Eq. **1** two preferentially selected wave vectors $k_y^{(s)} = -k_y^{(i)} \pm \delta k_y$ separated by $2\delta k_y \equiv 2/\delta y$ as suggested by the right column of Fig. 6. These two wave vectors lead to the interference of the signal photons despite the which-slit information.

This analysis shows that the interference fringes in Fig. 4 are a consequence of the TEM_{01} mode. Therefore, one might wonder if the mechanical double-slit is even necessary, especially because the one of the two slits is matched to the separation of the two intensity maxima of the mode. Moreover, our theoretical analysis does not contain the slits and we still obtain the fringes. Therefore, interference may be observable even without the double-slit but a substantial loss in contrast may occur.

Sorting Atoms by Coincidences. Our experiments measure the first-order and the second-order correlation function (19)

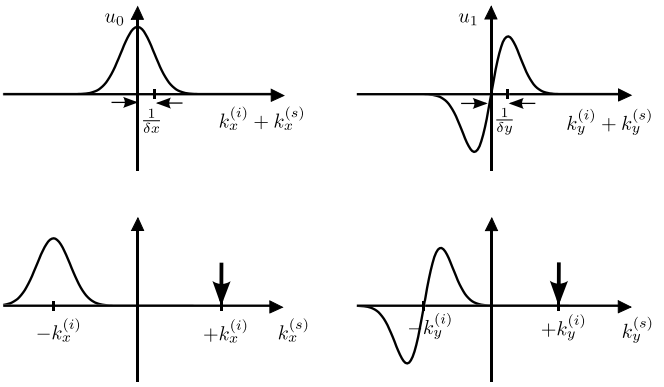

Fig. 6. Transverse wave vector components $k_x^{(s)}$ and $k_y^{(s)}$ of the signal photon determined from the measured values $k_x^{(i)}$ and $k_y^{(i)}$ (vertical arrows) of the transverse wave vector of the idler photon together with the lowest Hermite–Gauss mode functions $u_0[\delta x(k_x^{(s)} + k_x^{(i)})]$ and $u_1[\delta y(k_y^{(s)} + k_y^{(i)})]$. In the case of u_0 (left column) the values of $k_x^{(s)}$ are distributed according to the initial Gaussian around $-k_x^{(i)}$ with a single maximum and a spread $1/\delta x$. However for u_1 (right column) we find that the distribution of values of $k_y^{(s)}$ has two maxima separated from each other by $2/\delta y$ and located symmetrically around $-k_y^{(i)}$. The resulting two dominant wave vectors of the signal photon are the origin of the interference.

Downloaded from https://www.pnas.org by 3.238.227.73 on September 20, 2024 from IP address 3.238.227.73.

$$G^{(1)}(x^{(s)}) = \mathrm{Tr}[\hat{\rho}\hat{E}^{(-)}(x^{(s)})\hat{E}^{(+)}(x^{(s)})], \quad [2]$$

and

$$G^{(2)}(x^{(s)}, x^{(i)}) = \mathrm{Tr}[\hat{\rho}\hat{E}^{(-)}(x^{(s)})\hat{E}^{(-)}(x^{(i)})\hat{E}^{(+)}(x^{(s)})\hat{E}^{(+)}(x^{(i)})] \quad [3]$$

where $\hat{\rho}$ denotes the density operator of the radiation field. We assume the detection of a signal and an idler photon on D2 and D1 located at the positions $\mathbf{r}^{(s)}$ and $\mathbf{r}^{(i)}$ at the times $t^{(s)}$ and $t^{(i)}$, abbreviated by the space-time points $x^{(s)} \equiv (ct^{(s)}, \mathbf{r}^{(s)})$ and $x^{(i)} \equiv (ct^{(i)}, \mathbf{r}^{(i)})$, respectively, and c is the speed of light.

Moreover, we expand the positive and negative frequency components

$$\hat{E}^{(+)}(ct, \mathbf{r}) \equiv \sum_{\mathbf{q}} \mathscr{E}_q \hat{a}_{\mathbf{q}} \mathrm{e}^{-\mathrm{i}(|\mathbf{q}|ct - \mathbf{q}\cdot\mathbf{r})} \quad [4]$$

and

$$\hat{E}^{(-)}(ct, \mathbf{r}) \equiv \sum_{\mathbf{q}} \mathscr{E}_q \hat{a}^{\dagger}_{\mathbf{q}} \mathrm{e}^{\mathrm{i}(|\mathbf{q}|ct - \mathbf{q}\cdot\mathbf{r})} \quad [5]$$

of the electric field operator $\hat{E} \equiv \hat{E}^{(+)} + \hat{E}^{(-)}$ into plane waves of wave vector $\mathbf{q}$ and frequency $\omega \equiv c|\mathbf{q}|$. Here $\mathscr{E}_{\mathbf{q}}$, $\hat{a}^{\dagger}_{\mathbf{q}}$, and $\hat{a}_{\mathbf{q}}$ are the vacuum electric field and the creation and annihilation operators of the plane wave mode characterized by $\mathbf{q}$, respectively.

Following the technique introduced in ref. 20 we can derive analytical expressions for $G^{(1)}$ and $G^{(2)}$. Because the formulas are rather complex we do not present them here but rather emphasize that they reflect three basic facts: (*i*) The idler and the signal photons are emitted simultaneously. (*ii*) The emitting atoms leading to clicks at the two detectors for a fixed time delay $\Delta t \equiv t^{(s)} - t^{(i)}$ lie on a hyperboloid. (*iii*) The atoms radiating are located on the cross section between the pump mode and the hyperboloid.

These features ensure that in a single scattering event different atoms contribute to the near-field and the far-field coincidences. Indeed, the latter arise from the double-hump structure of the TEM_{01} mode, which excites two different domains of the atomic hyperboloid. The radiation emitted from these two distinct groups of atoms interferes as predicted by the theoretical analysis in ref. 10 and realized by the experiment of ref. 21 based on two ions stored in a Paul trap. This mechanism explains the surprising interference in the far-field coincidence counts.

In the near-field configuration the only atoms satisfying the coincidence condition are half-in-between the detectors and therefore sit on the node of the pump mode. Because the only atoms that could cause the appropriate clicks are not excited perfect correlations between signal and idler photon on the upper-upper and lower-lower slits emerge.

Noncommuting Operators. We conclude by noting that the principle of complementarity is often interpreted as a consequence of the noncommutativity of quantum mechanical operators. It is therefore an interesting problem to identify the noncommuting operators ruling our experiment. Unfortunately this question goes beyond the scope of the present article, but it suffices to say that in the context of the delayed-choice experiment (22) based on a Mach–Zehnder interferometer operators corresponding to properties such as "which-path" and interference have been given. It is interesting that the recent experiment (23) also analyzes such operators.

Comparison to Related Work

Under standard conditions of SPDC (17) no interferences appear in the first order correlation function $G^{(1)}$. However, interferences do emerge (24) in the second-order function $G^{(2)}$.

Likewise, in the quantum eraser (10, 11) the which-path information stored in the internal state of the atom (10) or in the state of one of two cavities (11) destroys the interference pattern of first order. However, when we erase this information the field fringes reappear in the correlation function of second order. Hence, $G^{(1)}$ consists of the incoherent sum of two intensity patterns whose identical modulations are shifted with respect to each other by $\pi/2$ as to create a distribution without modulation. The joint measurement expressed by $G^{(2)}$ selects one of these modulated patterns.

In contrast, our experiment displays oscillations already in $G^{(1)}$. Because in this case $G^{(1)}$ is the incoherent sum of the interference patterns $G^{(2)}$ corresponding to the signal photons in the far field conditioned on the idler photon on the upper and the lower intensity spots $G^{(2)}$ also shows oscillations.

Although this phenomenon is at the very heart of our experiment it is not the central point of our article. Instead, we emphasize the use of the additional information contained in the near-field correlations of $G^{(2)}$ together with the corresponding far-field interference fringes emerging in $G^{(2)}$, which brings to light the apparent violation of the naive interpretation of the principle of complementarity. We observe second order interferences by sorting the interfering signal photons according to their which-slit information stored in the idler photon.

Moreover, it is interesting to compare and contrast our experiment to ones (25, 26) that realize Einstein–Podolsky–Rosen (EPR) correlations (27) between the position and momentum variables of two particles by the quadrature operators of two entangled light fields. In contrast to these experiments we not only rely on the correlations between the field operators but also need the space dependence of the mode functions. This additional ingredient that constitutes the main difference between the quantum mechanics of two particles and the quantum theory of a field (28) stands out most clearly in the expressions Eqs. **2** and **3** for the correlation functions. Here not only the annihilation and creation operators $\hat{a}_{\mathbf{q}}$ and $\hat{a}^{\dagger}_{\mathbf{q}}$ appear through $\hat{E}^{(+)}$ and $\hat{E}^{(-)}$ given by Eqs. **4** and **5** but also the plane wave mode functions. In particular, the space dependence of the far-field interference pattern is not given by the momentum-like field variable as in two-particle quantum mechanics but by an interplay between the field operators and the mode functions.

Conclusions

Quantum theory is built on the celebrated wave-particle dualism. However, its consequences are often hidden behind an opaque curtain of formalism and emerge in the process of the measurement of a quantum system. Indeed, it is the click of a photo detector and the observation of a photo electron that determines the particle nature while the mode, in which this photon was prepared, governs its wave properties. In our experiment the simultaneous observation of the two physical entities "wave" and "particle" is possible due to the use not of a single photon but a correlated photon pair. Indeed we have used the detection of the idler photon in either the upper or the lower spot of the pump mode and the entanglement between the idler and the signal photon due to the process of their creation by SPDC to obtain information about the position of the signal photon without ever touching it. In this way we have been able to localize it within one of the spots of the double-hump structure of the TEM_{01} mode. Nevertheless, the complete mode function, including the second "unoccupied" hump, is still imprinted on the signal photon in form of a superposition of two distinct wave vectors giving rise to interference. This interpretation arises from our theoretical analysis within quantum theory.

However, we emphasize that even in our experiment the measurements of the which-slit information and interference still require mutually exclusive experimental arrangements. In order to observe the near-field coincidences shown in Fig. 3 the detector

Downloaded from https://www.pnas.org by 3.238.227.73 on September 20, 2024 from IP address 3.238.227.73.

D2 has to be just behind one of the slits, whereas the interference fringes of Fig. 4 emerge only when we move D2 far away from the slits. Nevertheless, we obtain with the help of the entanglement of the photons from the first measurement complete which-slit information and recall this knowledge when we record in the second experiment the interference fringes. However, the EPR discussion (3) or the delayed-choice experiment (22) have taught us that quantum objects do not have a reality independent of a measurement as summarized (29) by the phrase "one cannot consider quantum properties as being 'real,' in the sense of 'objective reality.'"

John A. Wheeler (3), paraphrasing Bohr, expressed this fact most vividly by saying "No elementary quantum phenomenon is a phenomenon until it is a recorded phenomenon brought to a close by an irreversible act of amplification."

In this sense our experiment can also be interpreted as another confirmation of the nonobjectifiability of quantum mechanics or, as stated by Torny Segerstedt, "Reality is theory."

Materials and Methods

In this section we first provide more information about the fit of the interference fringes of Fig. 4 and the experimental setup of Fig. 1. We then propose a model explaining the experimental results.

Modeling the Interference Fringes. We fit the interference fringes shown in Fig. 1 using the function

$$I(\zeta) = A + B\left(\frac{\sin\zeta}{\zeta}\right)^2 \frac{1}{2}[1 + C\cos\left(2\frac{a}{b}\zeta + \varphi\right)]. \qquad [6]$$

Here the free parameters A, B, C, and φ denoting the offset, the maximal interference signal, the spatial coherence and the phase shift, respectively, have been chosen as $A = 5$, $B = 35$, $C = 0.6$, and $\varphi \equiv 1.3\pi$. The dimensionless variable $\zeta \equiv \beta y$ is given by the product of the y coordinate and the scaling parameter $\beta \equiv b\pi/(\lambda f)$ consisting of the width b of the slits, the wave length λ of the light, and the focal length f of the lens. In our experiment these parameters take on the values $b = 60$ μm, $\lambda = 0.81$ μm, and $f = 75{,}000$ μm. Moreover, $a = 240$ μm is the separation of the two slits.

Detailed Description of Experimental Setup. In our experiment a single frequency diode laser from Toptica (Bluemode 405) in cw-operation with central wavelength 405 nm, output power 55 mW, and a diffraction limited beam quality served as the pump beam. The beam diameter was increased up to 5 mm using a telescope with lenses of focal lengths 25 mm and 200 mm, respectively. The TEM_{01} mode structure was generated using a spatial light modulator (SLM) as diffractive mirror. The SLM device from Holoeye was a phase-only modulator based on reflective liquid crystal on silicon micro display with $1{,}920 \times 1{,}080$ pixel resolution. The reflectivity of the SLM at a wavelength of 405 nm was about 50%.

After the SLM, a polarizer redefined the polarization direction of the pump light and a subsequent telescope formed by lenses of focal lengths 400 mm and 75 mm focused the beam into a BBO crystal cut for collinear phase matching of type II at 800 nm and thickness 2 mm. Inside the crystal the pump beam of 20 mW had a $1/e^2$ width and height of about 0.11 mm and 0.2 mm, respectively. Behind the crystal a mirror (antireflection coated at 810 nm, high-reflection coated at 405 nm) takes out the pump but lets the signal and idler photons pass. Moreover, filters were applied and a spectral bandwidth of 2 nm was realized at a peak wavelength of 810 nm.

The exit surface of the crystal was imaged on the double-slit with a photographical lens of focal length 50 mm and aperture 1.8. The horizontally arranged double-slit had a width of 60 μm and a slit separation of 240 μm. Thus at the slit the two spots of the TEM_{01}-mode structure were arranged vertically so that each of them illuminated just one of the slits. With a polarizing beam splitter the idler photon was coupled out and measured with the reference detector D1 at a distance from the crystal identical to that of the double-slit. With another single-photon counting detector D2 we either measure the near-field or the far-field region behind the double-slit. In the first case D2 behind the double-slit. In the second case we use a lens with focal length 75 mm in the f-f position between the double-slit and D2.

Wave Vector Correlations. In order to gain insight into the counterintuitive results of our experiments we next develop a model consisting of many three-level atoms being distributed homogeneously over space and being excited from their ground states by light in a given mode function $u = u(\mathbf{R})$. In this description we neglect for the sake of clarity the polarization degree of the electromagnetic field and assume that the excitation is weak so that there is only one atom excited at a time.

The atom decays from its excited to the ground state through a cascade—that is, by emitting the idler and signal photons of wave vectors $\mathbf{q}^{(i)}$ and $\mathbf{q}^{(s)}$, respectively. When the decay time of the intermediate state is short compared to the one of the excited state the two photons are entangled as expressed by the quantum state

$$|\Psi\rangle = N\sum_{\mathbf{R}} u(\mathbf{R}) \sum_{\mathbf{q}^{(i)},\mathbf{q}^{(s)}} c_{\mathbf{q}^{(i)},\mathbf{q}^{(s)}}(\mathbf{R})|\{1\}_{\mathbf{q}^{(i)}}, \{1\}_{\mathbf{q}^{(s)}}\rangle \qquad [7]$$

of the radiation field. Here $|\{1\}_{\mathbf{k}}\rangle$ denotes the photon number state of a single photon in the mode characterized by the wave vector $\mathbf{k}$, and all other modes are in the vacuum. Moreover, N is a factor that combines all constants relevant to the problem.

The coefficient $c_{\mathbf{q}^{(i)},\mathbf{q}^{(s)}}$ reflects the entanglement of the two photons in the modes $\mathbf{q}^{(i)}$ and $\mathbf{q}^{(s)}$ and contains (20), apart from a product of two coupled Lorentzians ensuring energy conservation of the two transitions, the position $\mathbf{R}$ of the atom through the mode function $\exp[-\mathrm{i}(\mathbf{q}^{(i)} + \mathbf{q}^{(s)}) \cdot \mathbf{R}]$ representing an outgoing plane wave. It is this factor that is crucial for the explanation of our experiment.

Indeed, the probability amplitude $\Psi = \Psi(\mathbf{k}^{(s)}; \mathbf{k}^{(i)})$ to obtain the signal photon with wave vector $\mathbf{k}^{(s)}$ given we have found the idler photon with $\mathbf{k}^{(i)}$ follows from $|\Psi\rangle$ defined by Eq. 7 as a discrete Fourier transform

$$\Psi(\mathbf{k}^{(s)}; \mathbf{k}^{(i)}) = \tilde{N}\sum_{\mathbf{R}} u(\mathbf{R})\mathrm{e}^{-\mathrm{i}(\mathbf{k}^{(s)}+\mathbf{k}^{(i)})\cdot\mathbf{R}} \qquad [8]$$

of the mode function u where $\tilde{N}$ is the product of N and the Lorentzians in $c_{\mathbf{q}^{(i)},\mathbf{q}^{(s)}}$.

We emphasize that the sum over the position $\mathbf{R}$ arises from the fact that we have a superposition of excitation paths. Indeed, every atom can be excited, but due to the weak excitation it is only one atom at a time. This feature is very much in the spirit of the model analyzed in ref. 10 where the diffraction of light from a double-slit has been replaced by the scattering from two atoms with internal structure. Moreover, the summation over $\mathbf{R}$ is also responsible (30) for the fact that the light spontaneously emitted from a gas of atoms propagates in the same direction as the excitation. However, in contrast to earlier work our interference effect arises from the mode function.

In order to connect this analysis with our experiment we consider the specific mode function

$$u(x, y, z) = u_T(x, y)\mathrm{e}^{\mathrm{i}k_z^{(p)}z} \qquad [9]$$

representing a propagation along the z axis with wave vector $k_z^{(p)}$ and transverse mode function u_T. We take the continuous limit of the distribution of atoms, which yields

$$\Psi(\mathbf{k}^{(s)}; \mathbf{k}^{(i)}) = N\int \mathrm{d}x \int \mathrm{d}y u_T(x, y)\mathrm{e}^{-\mathrm{i}(\mathbf{k}^{(s)}+\mathbf{k}^{(i)})\cdot\mathbf{R}_T} \times \int \mathrm{d}z \mathrm{e}^{\mathrm{i}(k_z^{(p)}-k_z^{(s)}-k_z^{(i)})z} \qquad [10]$$

with the transverse vector $\mathbf{R}_T \equiv (x, y)$.

Whereas the integration over z essentially ensures the conservation of the z components of the three wave vectors the Fourier transform of the transverse part u_T is responsible for the observed interference effect. Indeed, the probability amplitude $w(\mathbf{k}_T^{(s)}; \mathbf{k}_T^{(i)})$ to observe the transverse wave vector $\mathbf{k}_T^{(s)} \equiv (k_x^{(s)}, k_y^{(s)})$ of the signal photon given the transverse wave vector $\mathbf{k}_T^{(i)} \equiv (k_x^{(i)}, k_y^{(i)})$ of the idler photon follows from the Fourier transform $\tilde{u}_T$ of the transverse mode function $u_T = u_T(\mathbf{R}_T)$ with $\mathbf{R}_T \equiv (x, y)$ and reads

$$w(\mathbf{k}_T^{(s)}; \mathbf{k}_T^{(i)}) = \tilde{\alpha}\tilde{u}_T(\mathbf{k}_T^{(s)} + \mathbf{k}_T^{(i)}) \qquad [11]$$

where $\tilde{\alpha}$ is a constant.

We can represent the TEM_{01} mode of our pump beam of width δx and δy in the two transverse spacial dimensions by the product

Downloaded from https://www.pnas.org by 3.238.227.73 on September 20, 2024 from IP address 3.238.227.73.

$$u_T(x,y) = u_0\left(\frac{x}{\delta x}\right)u_1\left(\frac{y}{\delta y}\right) \quad [12]$$

of Hermite–Gauss functions

$$u_0(\xi) \equiv N_0 e^{-\xi^2/2} \quad \text{and} \quad u_1(\xi) \equiv 2N_1\xi e^{-\xi^2/2} \quad [13]$$

of dimensionless argument ξ and normalization constants N_0 and N_1.

When we recall that the Fourier transform $\tilde{u}_n$ of u_n is again given by u_n Eq. **11** leads us to Eq. **1**.

ACKNOWLEDGMENTS. We thank W. Becker, H. Carmichael, K. Dechoum, M. Freyberger, C. Henkel, M. Hillery, M. Komma, H. Paul, M.J.A. Spähn, and M. Wilkens for many fruitful and stimulating discussions. We are also most grateful to the referees for their constructive remarks that have led to a substantial improvement of our article.

1. Young T (1802) On the theory of light and colours. *Phil Trans R Soc London* 92:12–48.
2. Newton I (1730) *Opticks or a Treatise of the Reflections, Refractions, Inflections and Colors of Light*, (Printed for William Innys at the West-End of St. Paul's), Vol. 4.
3. Wheeler JA, Zurek WH (1984) *Quantum Theory and Measurement* (Princeton Univ Press) p 945.
4. Feynman RP (1948) Space-time approach to non-relativistic quantum mechanics. *Rev Mod Phys* 20:367–387.
5. Aharonov Y, Zubairy MS (2005) Time and the quantum: Erasing the past and impacting the future. *Science* 307:875–879.
6. Kocsis S, et al. (2011) Observing the average trajectories of single photons in a two-slit interferometer. *Science* 332:1170–1173.
7. Wooters WK, Zurek WH (1928) Complementarity in the double-slit experiment: Quantum nonseparability and a quantitative statement of Bohr's principle. *Phys Rev D Part Fields* 121:580–590.
8. Heisenberg W (1927) Über den anschaulichen Inhalt der quantentheoretischen Kinematik und Mechanik. *Z f Phys* 43:172–198 For an English translation see ref. 3.
9. Storey P, Tan S, Collett M, Walls D (1994) Path detection and the uncertainty principle. *Nature* 367:626–628.
10. Scully MO, Drühl K (1982) Quantum eraser: A proposed photon correlation experiment concerning observation and "delayed choice" in quantum mechanics. *Phys Rev A* 25:2208–2213.
11. Scully MO, Englert BG, Walther H (1991) Quantum optical tests of complementarity. *Nature* 351:111–116.
12. Dürr S, Nonn T, Rempe G (1998) Origin of quantum-mechanical complementarity probed by a "which-way" experiment in an atom interferometer. *Nature* 395:33–37.
13. Kim YH, Yu R, Kulik SP, Shih YH, Scully MO (2000) A delayed choice quantum eraser. *Phys Rev Lett* 84:1–5.
14. Bohr N (1928) The quantum postulate and the recent development of atomic theory. *Nature* 19:473–484.
15. Englert BG (1996) Fringe visibility and which-way information: An inequality. *Phys Rev Lett* 77:2154–2157.
16. Scully RJ (2007) *The Demon and the Quantum* (Wiley-VCH, Weinheim, Germany).
17. Boyd RW (1992) *Nonlinear Optics* (Academic, Burlington, MA).
18. Ostermeyer M, Korn D, Puhlmann D, Henkel C, Eisert J (2009) Two-dimensional characterization of spatially entangled photon pairs. *J Mod Opt* 56:1829–1837.
19. Glauber RJ (2007) *Quantum Theory of Optical Coherence* (Wiley-VHC, Weinheim, Germany).
20. Scully MO, Zubairy MS (1997) *Quantum Optics* (Cambridge Univ Press, Cambridge, UK).
21. Eichmann U, et al. (1993) Young's interference experiment with light scattered from two atoms. *Phys Rev Lett* 70:2359–2362.
22. Hellmuth T, Walther H, Zajonc A, Schleich W (1987) Delayed-choice experiments in quantum interference. *Phys Rev A* 35:2532–2541.
23. Liu HY, et al. (2012) Relation between wave-particle duality and quantum uncertainty. *Phys Rev A* 85:022106.
24. Gosh R, Mandel L (1987) Observation of nonclassical effects in the interference of two photons. *Phys Rev Lett* 59:1903–1905.
25. Howell JC, Bennink RS, Bentley SJ, Boyd RW (2004) Realization of the Einstein-Podolsky-Rosen Paradox using momentum- and position entangled photons from spontaneous parametric down conversion. *Phys Rev Lett* 92:210403.
26. Leuchs G, Dong R, Sych D (2009) Triplet-like correlation symmetry of continuous variable entangled states. *New J Phys* 11:113040.
27. Einstein A, Podolsky B, Rosen N (1935) Can quantum-mechanical description of physical reality be considered complete? *Phys Rev* 47:777–780.
28. Fermi E (1932) Quantum theory of radiation. *Rev Mod Phys* 4:87–132.
29. Paul H (2008) *Quantum Theory* (Cambridge Univ Press, Cambridge, UK).
30. Scully MO, Fry ES, Ooi CHR, Wódkiewicz K (2006) Directed spontaneous emission from an extended ensemble of N atoms: Timing is everything. *Phys Rev Lett* 96:010501.

Downloaded from https://www.pnas.org by 3.238.227.73 on September 20, 2024 from IP address 3.238.227.73.